Analysis of Micro-mechanical Damage in Tool Steels Coupling Fracture Tests and Acoustic Emission

Ingrid Picas[1,a], Eva Martínez-González[2,b], Daniel Casellas[1,3,c] and Jordi Romeu[2,d]

[1] Fundació CTM Centre Tecnològic, Av. Bases de Manresa 1, 08242 Manresa, Spain

[2] Laboratori d'Enginyeria Acústica i Mecànica (LEAM), Universitat Politècnica de Catalunya (UPC), EUETIB, Urgell 187, 08036 Barcelona, Spain

[3] Departament de Ciència dels Materials i Enginyeria Metal·lúrgica (CMEM), Universitat Politècnica de Catalunya (UPC), EPSEM, Av. Bases de Manresa 61, 08242 Manresa, Spain

[a] ingrid.picas@ctm.com.es, [b] eva.martinez-gonzalez@upc.edu, [c] daniel.casellas@ctm.com.es, [d] jordi.romeu@upc.edu

Keywords: Microstructure, micro-mechanics, damage, signal, failure.

Abstract. Fracture tests and Acoustic Emission (AE), a technique providing wave-like information, were coupled in this study in order to obtain in-situ data characterization of damaging mechanisms. Characteristic AE signals, i.e. waves with different energy, frequency, amplitude, etc., were analyzed and related to micro-mechanical and damaging mechanisms taking place in the microstructure. The occurrence of these signals varied depending on the considered steel in terms, for instance, of the quantity of registered signal or the stress at which they started to be recorded. The results of this investigation permitted to set the stresses at which crack nucleation and propagation processes started to occur in two tool steels with very different microstructural properties, and they provided very helpful information to understand the failure mechanisms acting in these steels.

Introduction

One of the outcomes of the increasing environmental and passenger safety regulations in cars, together with the global concern of exhausting fossil fuel resources, is the construction of lightweight vehicles with increased crash resistance. New and advanced materials are currently under development to satisfy the underlying demands on vehicles. However, implementing with success these materials in body-in-white and chassis components requires optimization of the routes by which they are to be manufactured. Among the factors interfering with the viability of producing such components, the premature failure of tools is one of the most important -directly reflecting- the final price of manufactured parts. Thus, understanding the fracture events of tools is crucial to foresee tool lifetime and to further develop tool steels with improved mechanical performance.

The interaction between the two main constituents of tool steel microstructures: the primary carbides and the metallic matrix, determines their mechanical properties and hereby, the performance of tools working in industrial applications. A proper comprehension of the micro-mechanical mechanisms leading to damage in the microstructure prior to failure comprises the identification, localization and quantification of the phenomena being involved in the process when a certain load is applied.

In order to reach this goal, an innovative field-based approach was undertaken in this work, combining fracture tests with Acoustic Emission (AE) monitoring and wave signal analysis. Despite

AE is a well known technique for non-destructive inspection, only scarce data exist in the literature concerning its application for the analysis of micro-damage of tool steels. Fukaura et al. [1] and Yokoi et al. [2] are amongst the few authors who employed this technique to test two tool steels in order to determine the progression of internal damage. The steels used were JIS SKD11 (an equivalent steel type to DIN 1.2379 or AISI D2) and a modified SDK11 with reduced Cr and C content and increased Mo and V. AE signals from carbide cracking could successfully be detected by these authors; the signals started at a certain applied load and the event rates continually increased until reaching the fracture stress. These authors stated that no continuous AE signals existed, but that numerous burst emissions at close intervals were recorded instead.
Martínez-González et al. [3] showed that three different zones could be distinguished during a bending test in a tool steel sample with regard to the AE events. In the first zone, almost no signals were detected and it neither did any damage at the microstructure. In the second zone, AE signals started to be recorded and they increased gradually in intensity and abruptly in number. During this stage, several broken carbides were discerned at the surface by means of optical microscopy due to the increase of applied stress during the test. Finally at the third zone, the amount of AE signal as well as the cumulative energy increased considerably. At this stage, many cracks were observed to propagate at the microstructure.
A better understanding of the correlation between AE signals and micro-damage in monotonic conditions was given by Yamada and Wakayama [4]. Although these authors used AE monitoring to clarify the flexural fracture of cermets, they observed a rapid increase in cumulative AE energy prior to the final fracture and attributed this phenomenon to the main crack formation. They also distinguished two types of AE signal: one was a burst-type signal with high frequency and the other was a low frequency and continuous-type signal. The former was considered to be emitted from micro-cracking while the latter was due to plastic deformation of the binder phase.
From this standpoint, this work deals with the coupling of AE techniques to mechanical tests, namely a three point bending test, in case of tool steels with different microstructural features in terms of size, geometry and distribution of primary carbides in the metallic matrix. The main focus here is the study of damage events under monotonic loading and obtaining net waves associated with each one of them.

Experimental Procedure

Two different cold work tool steels were considered in this study. The first type is a conventional ledeburitic high-carbon, high-chromium tool steel DIN 1.2379 (AISI D2). The second is a special grade of cold work tool steel developed by ROVALMA S.A., named HWS, which in comparison to the aforementioned 1.2379 has lower carbon and chromium content but higher of vanadium. 1.2379 is obtained by ingot metallurgy routes while HWS is produced by powder metallurgy. The main alloying elements found in their chemical composition are shown in Table 1.

Table 1. Main alloying elements in the chemical composition of the studied steels (in wt %)

Steel	C	Cr	Mo	W	V
1.2379	1.5-1.6	11.0-12.0	0.6-0.8	-	0.9-1.0
HWS	0.9-1.2	6.8-8.5	-	1.1-1.4	2.5-3.0

Prismatic samples were extracted from forged and annealed commercial bars parallel to the forging direction. Heat treatment was applied to the samples of each material in order to get a hardness level of 60 – 62 HRC, as summarized in Table 2. The bending strength, σ^R, of these materials was reported by Picas et al. [5], and the fracture toughness, K_{IC}, was determined as specified in the ASTM E 399-90 standard. These values are also showed in Table 2.

Table 2. Heat treatment applied to the studied materials and obtained hardness and bending strength

Steel	Austenitizing (quench in oil)	Tempering	HRC	σ^R [MPa] [5]	K_{IC} [MPa·m$^{1/2}$]
1.2379	1050 ºC for 30 min	550 ºC for 2 h (x2)	60 - 62	2847 ± 96	28
HWS	1060 ºC for 35 min	540 ºC for 2 h (x3)	60 - 62	4382 ± 111	21

Fracture tests were performed by means of three point bending tests with a constant span length of 40 mm. Samples dimensions were 8 mm x 6 mm x 120 mm. Samples were mechanically ground and their corners were rounded to avoid stress magnifications and remove any defect introduced during sample preparation. Faces subject to tensile stress during three point bending tests were carefully polished to mirror-like using colloidal silica particles with approximately 40 nm sizes.
Microstructural inspection of the samples was carried out using a FE-SEM (Field Emission Scanning Electron Microscope) and the fracture tests were performed in a universal testing machine using an articulated fixture to minimize torsion effects. The applied displacement rate was 0.01 mm/min.
The test was monitored using sensors of a fixed resonance frequency of 700 kHz (VS700D, Vallen System GmbH) and three pre-amplifiers with a 34 dB gain of the same brand were also used (AEP4). Acoustic Emission (AE) signals were recorded and analyzed using the Vallen Systeme GmbH AMSY5 analyzer. The experimental set-up is schematized in Fig. 1.

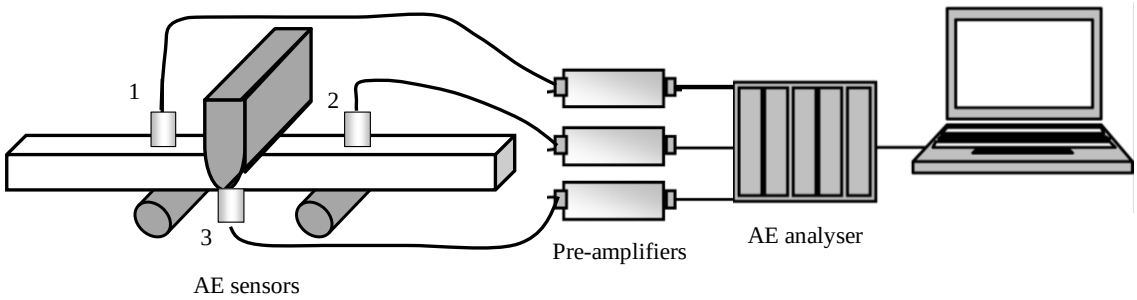

Fig.1. Experimental set-up for the AE-monitored bending tests.

During the measurements, digital filters of 95-850 kHz were applied. Very short signal acquisition times (s) were chosen in order to avoid capturing noise produced by the rebounding of the waves due to surface walls. Furthermore, only the initial part of every signal was considered as purely representative of micro-damage phenomena.
Using this set-up configuration, 3 to 5 samples of each material were monitored until final fracture. Later, 2 to 3 samples were analyzed by means of stepwise loading (Fig. 2a)) in order to relate each type of AE characteristic signal pattern to the generated damage in the microstructure. Surface inspection of samples was carried out after each load increment in a Confocal Microscope (CM) (Fig. 2b)).

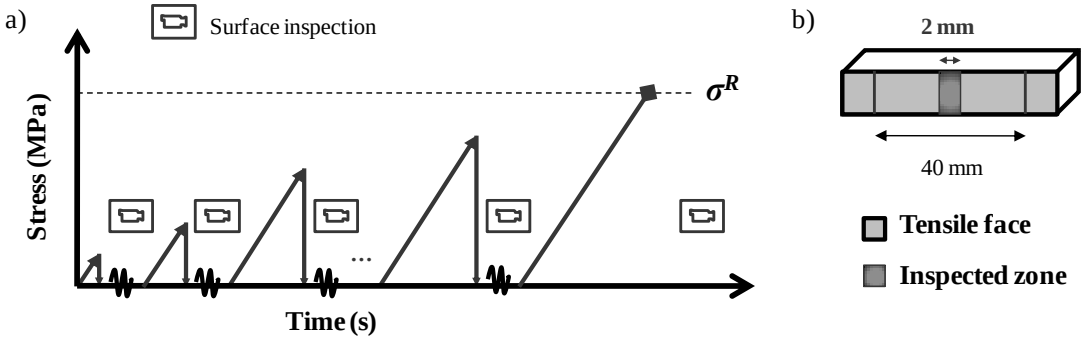

Fig.2. a) Stepwise loading to final fracture of the sample, σ^R; b) schema of the micrographically inspected zone of samples.

Results

Microstructural Analysis. In Fig. 3 the microstructure of the steels studied can be observed. The microstructure of 1.2379 (Fig. 3 a)) was markedly anisotropic, with large carbide stringers forming bands in the metallic matrix. The primary carbides of this steel were rather large and had irregular morphologies. HWS showed the typical microstructure of PM steels (Fig. 3 b)) with very small spherical carbides distributed in the matrix with no preferred orientation.

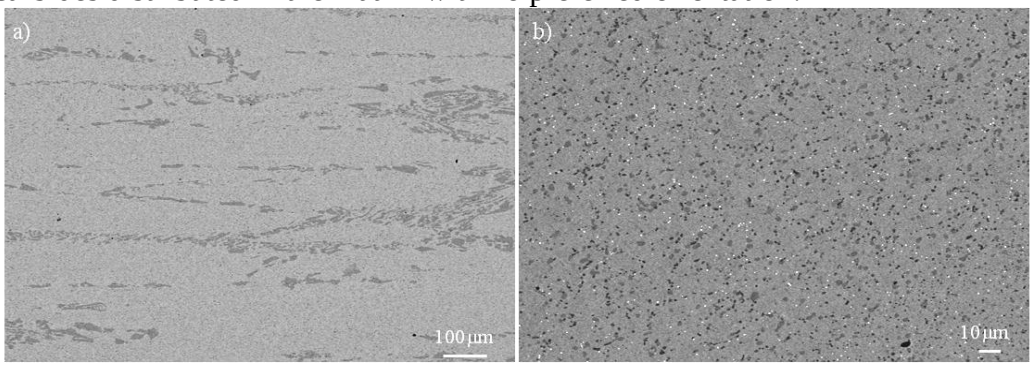

Fig.3. Microstructure of the studied tool steels: a) 1.2379, b) HWS.

Identification of Characteristic AE Signal Patterns in Bending Tests of 1.2379 under Monotonic Loading. Fig.4 a) shows the results of the AE signals registered in bending tests under monotonic loading for 1.2379. This diagram plots the cumulative number of hits in function of the stress applied and the location of each signal on the sample surface (with respect to the centre of the sample). As it can be observed, the highest amount of signals was generated at the centre of the sample (X-Loc. = 0 in Fig 4a), where the applied stress was the highest during the three point bending test, and the quantity of emitted signal continuously increased with the applied stress.

A closer gaze to the AE signals obtained allowed to classify them into two categories depending on their characteristic patterns. As shown in Fig.4 b), at the beginning of the test, no AE signals were detected. At a certain applied stress level, a first type of AE signal started to be recorded (green line in Fig.4 b)). These signals were not continuous but they were emitted in a burst-like manner, and the quantity of hits registered increased along with the applied stress. Later as the stress increased, a second type of signal was distinguished (red line in Fig.4 b)). This signal also increased in number of hits together with the applied stress, but at the moment of final fracture it attained lower hit values than the first signal type.

These two signals identified not only differed because of the number of hits, but also they had very different characteristic frequencies and waveforms. As shows Fig.4 c), the first type of signal had a main frequency of 280 kHz, while the frequency of the second type was around 650 kHz. These

different frequency ranges of the two signals indicated that the responsible mechanisms for emitting them took place at different velocities in the microstructure, i.e. the second mechanism would be much faster than the first one.3

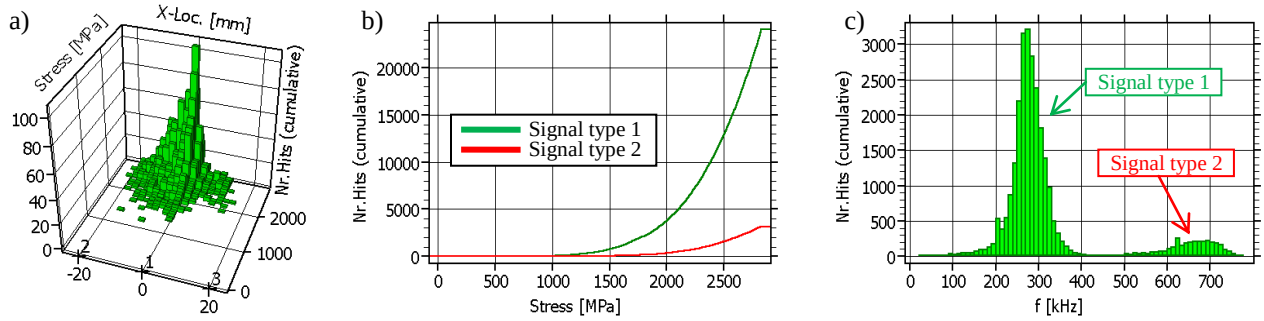

Fig.4. a) Cumulated number of hits in function of the stress applied during the bending test and the location of the signals at the sample surface (the X axis (X-Loc.) refers to the position of the signal with respect to the sample centre, the Y axis refers to the applied stress and the Z axis to the cumulated number of hits registered); b) cumulated number of hits vs applied stress during a monotonic bending test in which two different types of AE signals could be identified; c) cumulated number of hits vs frequency for the two signals registered.

Relationship between AE Signals and Micro-Damage during Bending Tests of 1.2379 under Monotonic Loading. Stepwise bending tests permitted to inspect the tensile surface of the samples at different increasing stress levels, and correlate the registered AE data (namely the two different identified signal types) to the micro-damage observed in the microstructure.

In Fig.5 a) the cumulated number of hits in function of the stress applied at the first load step can be observed. This test was stopped at 800 MPa, in the moment in which the first signals were detected. These signals answered to the same pattern than those of type 1 identified before. However, no damage could be observed at the sample surface, as shown in Fig. 6 a); likely something happened at the microstructure but it could not be detected yet.

The next test was stopped at 2200MPa, when a higher quantity of AE signal was detected. Practically all signals responded to the characteristics of the type 1 identified before, and few hits of characteristic type 2 signals were first detected (Fig. 5 b)). In this case, the first cracks were observed in the microstructure and they were located at primary carbides (Fig. 6 b) and c)). However and despite many carbides were broken, none of the cracks nucleated from them were observed to have started propagating through the metallic matrix surrounding the broken carbide.

The last load step at 2600 MPa revealed a notable increase of the type 2 signal, even though the number of hits of the type 1 had not ceased to increase (Fig.5 c)), as well as the number of broken carbides in the sample. The inspection of the surface permitted to observe that some cracks had now propagated through the metallic matrix (Fig.6 d)).

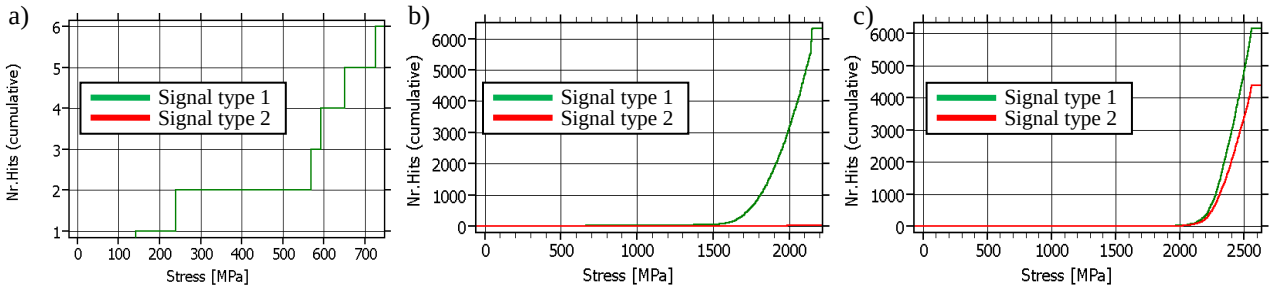

Fig.5. AE signal results of monotonic stepwise tests in 1.2379 in terms of the cumulated number of hits vs applied stress to: a) 800 MPa; b) 2200 MPa and c) 2600 MPa.

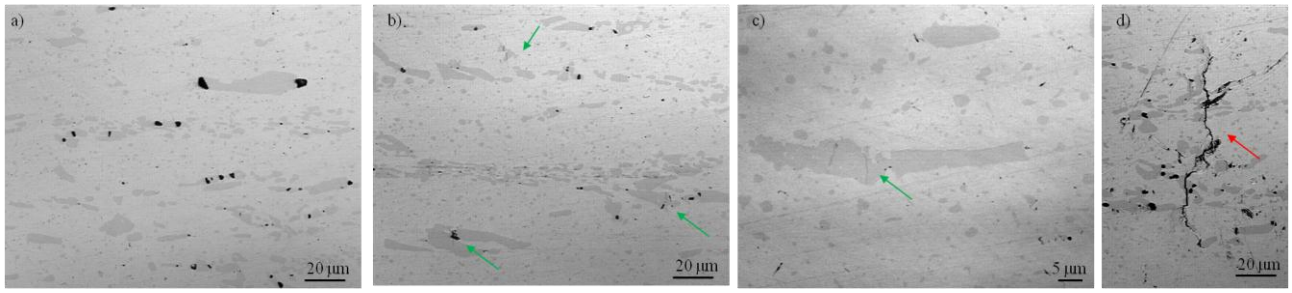

Fig.6. Images of the microstructure of 1.2379 at: a) 800 MPa; b)-c) 2200 MPa and d) 2600 MPa.

As it followed from the obtained results, the first and the second AE signal types were related to different damage mechanisms occurring in 1.2379 samples as the applied stress increased. The first type of signal corresponded to the breakage of carbides in the microstructure, i.e. nucleation of cracks, while the second type was emitted by the subsequent propagation of these cracks through the metallic matrix.

Relationship between AE Signals and Micro-Damage during Bending Tests of HWS under Monotonic Loading. As shown in the previous lines, coupling the AE sensors to the bending test permitted identify the different micro-mechanical mechanisms leading to failure; i.e. in 1.2379 the acquisition of AE signals was directly related to the occurrence of crack nucleation and propagation processes in the microstructure.

In case of HWS however, only a few AE signals could be detected when performing the same analysis as in 1.2379, even when the threshold established for noise amplitudes was reduced to lower values. Fig. 7 a) and b) show the cumulated number of hits in function of the applied stress for stepwise tests of HWS at 3300 and 4100 MPa respectively. In this figures it can be observed that the first signals were registered at 1700 MPa but just a few hits were detected and that they mostly corresponded to the signals of type 1. However, given that only these few amounts of signals were detected, and that the microstructural size of HWS is very small, no cracks could be observed at the surface at 3300 MPa (as shown in Fig. 8 a) using the maximum magnifications possible in the confocal microscope). However, when the load was increased to 4100 MPa, Fig. 8 b) and c) show that very few and small cracks were nucleated at the microstructure, both at broken primary carbides and inclusion particles.

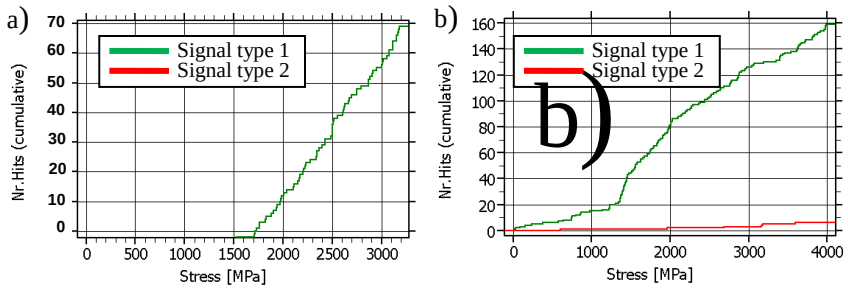

Fig.7. AE signal results of monotonic stepwise tests in HWS in terms of the cumulated number of hits vs applied stress to: a) 3300 MPa and b) 4100 MPa.

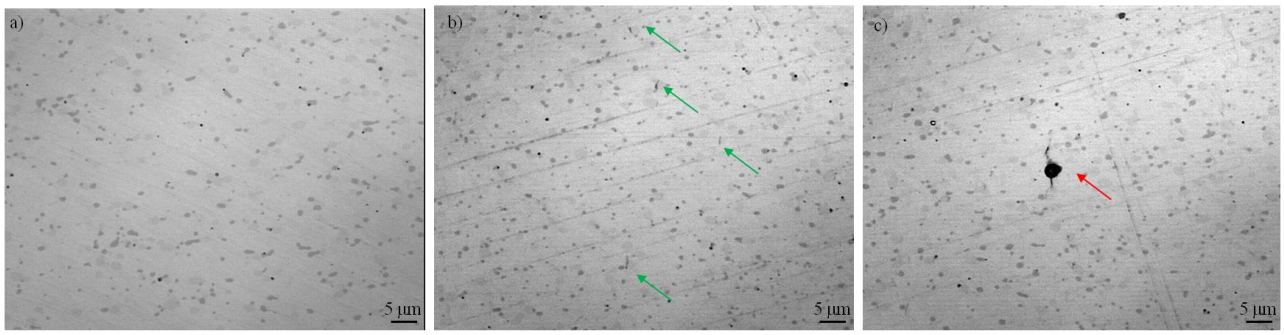

Fig.8. Images of the microstructure of HWS at: a) 3300 MPa and b) an c) 4100 MPa.

Discussion

The data shown above these lines permitted to corroborate that the AE technique, coupled to the bending tests under monotonic conditions, was able to provide accurate information regarding the acting micro-mechanical and damaging mechanisms of 1.2379. In this case, the nucleation and propagation of cracks in the microstructure was well identified by means of two different types of AE signals reporting respectively, the breakage of carbides in the microstructure, i.e. the nucleation of cracks, and the moment when these cracks left the carbide an grew through the metallic matrix, i.e. the propagation of cracks. Therefore, this technique provided a unique and very accurate tool to determine the threshold stresses at which carbides started to break and hereby, the stresses at which the first cracks were nucleated.

In case of HWS, it was found that even though the first signals started at 1700 MPa, only very few hits were registered compared to the high amounts obtained with 1.2379. These signals corresponded to the type 1 ones and therefore, in correlation to what it was observed in 1.2379, some cracks were expected to have nucleated in the microstructure. However, no damage could be identified at the surface until a stress of about 4000 MPa was applied. At that moment, very small cracks were detected in primary carbides and inclusions. It is worth to say that practically no signals of type 2 were recorded before the final fracture of the sample; as neither did any propagation of cracks. This meant that the very high fracture resistance of HWS was mainly due to the contribution of a very high resistance to crack nucleation, but that the propagation of the nucleated cracks to final fracture took place very rapidly (in a very brittle-like manner).

In order to shed light to an explanation of this phenomenon, the concepts of Linear Elastic Fracture Mechanics were used. According to Eq.1, under such high applied stresses, σ, as those sustained by HWS (e.g. 4000 MPa), it is reasonable to say even if a very small crack is nucleated at a carbide or inclusion in the microstructure (very small a value, e.g. 5 µm), the acting stress intensity factor, K, of this crack can already attain close values to those of the fracture toughness of the material, K_{IC}, (K = 11 MPa·m$^{1/2}$ assuming Y = 1,2 while K_{IC} is 21 MPa·m$^{1/2}$). Furthermore many cracks are nucleated at such stress levels and thus, coalescence of these cracks is prone to occur and rapidly lead to fracture.

$$K = Y\sigma\sqrt{a} \qquad (1)$$

In 1.2379 the first cracks were nucleated at much lower stress values (e.g. 1500 MPa) in the large primary carbides embedded in this steel (higher a values, e.g. 15 µm), but as shows Table 2, the K_{IC} of 1.2379 is higher than that of HWS (28 vs 21 MPa·m$^{1/2}$ respectively). Thus, cracks may propagate to longer lengths before critical failure takes place (their K = 7 MPa·m$^{1/2}$ and should reach K_{IC} 28 MPa·m$^{1/2}$), and they would be easier to be identified both by visual inspection of the surface and by means of AE techniques. In addition, the much larger primary carbides of 1.2379 compared to HWS propitiated that cracks were nucleated at the surface (where the stresses during the three points bending test are maxima) instead of inside the material (as it could have been the case if there was a

sufficiently large inclusion in the interior of an HWS sample). Therefore, cracks in 1.2379 would always be observed by surface inspections, while those of HWS would not.
In any case, the results obtained in the present study suggested that further work should be devoted to characterize the fracture phenomena in steels with very fine microstructures as powder metallurgy tool steels. The findings of this investigation were not enough to clarify whether cracks really nucleated in the microstructure of this steel at stresses around 1700 MPa or the AE technique introduced in this work failed at detecting the initial stress level for crack nucleation in HWS samples.
The fact that only very few AE activity was detected in tests with HWS, and taking into account the small sizes of the nucleated cracks, brought to mind the question of whether the generated signals were under the working amplitudes of the sensors. Further improvement of the present work will consider the use of sensors specially adapted for low amplitude signals in case of testing with HWS, so that any possible signal coming from the microstructure can be analyzed.

Summary

The method developed in this study by which bending fracture tests were coupled to AE techniques provided helpful results to understand in great detail the failure mechanisms of tool steels under such applied loading, as well as the interaction of their microstructural constituents. Two different tool steels were analyzed by this means, both showing very different microstructural features such as the size, geometry and distribution of the primary carbides embedded. The first of the steels studied, 1.2379, permitted to identify two different AE signal wave patterns during a fracture test. These signals were respectively assigned to crack nucleation in primary carbides, and the propagation of these through the metallic matrix. The second of the studied materials, HWS, showed a very fine microstructure with very small carbides distributed homogeneously in the matrix. In this steel, some AE signals related to the type 1 ones started to be detected at a certain applied load, but no damage could be observed at the surface of the sample until much higher applied stresses were applied. Type 2 AE signals were practically inexistent in this material, but any propagation of cracks could neither be detected. An analysis from the point of view of fracture mechanics permitted to understand the reason why such different behaviors were observed in these two materials. However, further work is required in order to rationalize the AE pattern obtained in HWS, and for that, new sensors with reduced working amplitude will be employed in order to ensure that a more accurate detection of the phenomena taking place in the microstructure is performed.

Acknowledgements

Authors from Fundació CTM Centre Tecnològic acknowledge the Catalan government for partially funding this work under grant TECCTA11-1-0006.

References

[1] K. Fukaura and K. Ono: J. Acoustic Emission Vol. 19 (2001), p. 91
[2] D. Yokoi, N. Tsujii and K. Fukaura: Mat. Sci. Res. Int. Vol. 9:3 (2003), p. 216
[3] E. Martínez-González, I. Picas, D. Casellas and J. Romeu: J. Acoustic Emission Vol. 28 (2010), p. 163
[4] K. Yamada and S. Wakayama: *AE Monitoring of Microdamage during Flexural Fracture of Cermets* (Euro PM2009, Copenhagen, Denmark), (October 2009), p. 247
[5] I Picas, R. Hernández, D. Casellas and I. Valls: *Strategies to Increase the Tool Performance in Punching Operations of UHSS* (50th IDDRG Conference, Graz, Austria) (June 2010), p. 325